Electrical and mechanical properties of intrinsically flexible and stretchable PEDOT polymers for thermotherapy

Amélie Schultheiss, Amélie Revaux, Alexandre Carella, Martin Brinkmann, Huiyan Zeng, Renaud Demadrille, Jean-Pierre Simonato

Electrical and Mechanical Properties of Intrinsically Flexible and Stretchable PEDOT Polymers for Thermotherapy

Amélie Schultheiss,[1] Amélie Revaux,[1,*] Alexandre Carella,[1,*] Martin Brinkmann,[3] Huiyan Zeng,[3] Renaud Demadrille,[2] Jean-Pierre Simonato,[1,*]

[1] Univ. Grenoble Alpes, CEA, LITEN/DTNM, F-38000 Grenoble, France

[2] Univ. Grenoble Alpes, CEA, IRIG, SYMMES, F-38000 Grenoble, France

[3] Univ. Strasbourg, CNRS, ICS UPR 22, F-67000 Strasbourg, France

Email addresses: amelie.revaux@cea.fr; alexandre.carella@cea.fr, jean-pierre.simonato@cea.fr

Abstract

For wearable applications such as electronic skin and biosensors, stretchable conductors are required (~30% strain to follow the skin extension). Owing to its high conductivity, good flexibility, low-cost, and ease of processing, poly(3,4-ethylenedioxythiophene) (PEDOT) appears as a promising candidate. However, destructive cracks come out above 10% strain in the case of PEDOT:PSS, the most common form of PEDOT. Different strategies have already been investigated to solve this problem, including the design of specific structures or the addition of plasticizers. This article presents a different approach to obtain highly conductive and stretchable PEDOT materials, based on doping with small counter-anions. We indeed demonstrate the intrinsic stretchability (up to 30% strain) of thin films (35 nm) of PEDOT-based materials with small counter-ions. Both thin-PEDOT:OTf (triflate counter-ion) and thin-PEDOT:Sulf (sulfate counter-ion) films remain structurally resilient up to 25–30% strain, and

their electrical conductivity remains remarkably stable over more than 100 cycles. Under limited strain (< 30%), polarized UV-Vis-NIR measurements (parallel and perpendicular to the stretching direction) show that the conductivity of the material is improved by chain alignment in the stretching direction. As a proof of concept, a thermotherapy patch is presented. It shows a fine temperature control (stability around 40°C at 9 V bias) and a uniform heating across the surface.

I. Introduction

Organic electronics have become increasingly attractive in recent years, chiefly thanks to the availability of easily processed, lightweight organic materials with good mechanical properties. The most widely used conductive polymer, poly(3,4-ethylenedioxythiophene) (PEDOT), can be engineered to have a conductivity higher than 5000 $S \cdot cm^{-1}$,[1–5] while its polymeric nature makes it highly flexible and suitable for wearable devices.[6–8] For certain applications however, such as electronic skin and wearable biosensors, stretchability is also required.[9–11] The most common form of PEDOT is the PEDOT:PSS, with a polystyrene sulfonate (PSS) counter-anion, notably because of its commercial availability. Although it is intrinsically slightly flexible, destructive cracks appear above 10% strain.[12,13] There are different possible strategies to make conducting materials stretchable or improve their stretchability. The first is to use a specific structure or design (wavy, buckling, meandering or serpentine), for example by depositing the conductive material on a pre-strained (pre-stretched) elastomeric substrate. The second approach is to increase the stretchability of the

material itself by adding plasticizers.[14–17] For PEDOT:PSS, a variety of plasticizers have been tested including surfactants [12,18–21], ionic liquids,[22–24] polymers [25,26] and biocompatible compounds such as d-sorbitol.[27]

This article presents a different approach to obtain highly conductive and stretchable PEDOT, based on doping with small counter-anions. In PEDOT:PSS indeed, the PSS phase predominates and prevents the polymer chains from easily sliding past each other during stretching. Here, we report on the mechanical properties of two PEDOT-based materials, with either a triflate counter-ion (PEDOT:OTf) or a sulfate/hydrogen sulfate counter-ion (PEDOT:Sulf). The PEDOT in this work is synthesized with short chains (a few tens of units) and small counter-ions, with a form and morphology that have been investigated through X-rays diffraction and AFM (Atomic Force Microscopy) measurements on glass substrate.[1,2] Such PEDOT materials were shown to be highly flexible and able to keep excellent electrical performances even after hundreds of cycles when deposited on polymeric substrates.[28] For both counter-anions, two different film structures were evaluated *thick-PEDOT* films (500 nm thick) and *thin-PEDOT* films (30–35 nm thick). The goals of this study were to investigate the interplay between electrical and mechanical properties in these PEDOT materials, and to demonstrate their intrinsic stretchability and suitability for use in heat patches. The requirement in this context is that the sheet resistance should be maintained at a similar level up to strains of at least 30%, the maximal strain imparted by knee flexion.[26,29]

When interpreting resistance/strain curves, it is important to remember that increases in resistance may simply be due to changes in the shape of the sample, through the Poisson effect, rather than to a drop in conductivity. The Poisson effect (directly related to the Poisson ratio, ν, of the substrate–conductive film material), namely the transverse contraction of the sample (decrease in width, w, and thickness, t) during axial elongation

(increase in length, L). The expression for the relative resistance of the material, R/R0, as a function of the strain is:

$$\frac{R}{R0}(\varepsilon_L) = \frac{(1+\varepsilon_L)}{(1+\varepsilon_w)(1+\varepsilon_t)} = (1+\varepsilon_L)^{1+\nu_w+\nu_t} \qquad (1)$$

with ε_w, ε_t and ε_L the changes in width, thickness, and length of the conductive film, and ν_w and ν_t the associated Poisson ratios.

This equation was derived from the Poisson ratio equation, as described by He et al.[27] The change in relative resistance R/R0 of the material due to Poisson effect can be plotted as a function of the strain (**Figure S1**). Here, the Poisson ratio of the substrate (styrene–ethylene/butylene–styrene, SEBS) has been used for ν_w (= 0.499) [30] and the one of PEDOT:PSS for ν_t (= 0.350) [31], as described by He et al.[27]

The change in resistance as a function of the strain was measured using a custom test bench with a specific mask and frame for the samples (**Figure 1**.a). The main advantage of this setup is that the electrical contact is not taken under the clamps, which avoids contact loss during stretching. This setup also allowed two samples to be tested simultaneously, allowing their behaviors to be compared accurately under identical strains and strain rates.

II. Results and Discussion

We first compared the properties of *thick-PEDOT:OTf (OTf = triflate counter-ion)* samples prepared in either straight or wavy lines (**Figure 1**.a), to evaluate the effect of the design. To compare the electrical behavior of the two configurations (straight and wavy) under strain,

the resistance of the samples was continuously measured over five cycles from 0% to either 10% and 30% strain (**Figure 1**.b,c).

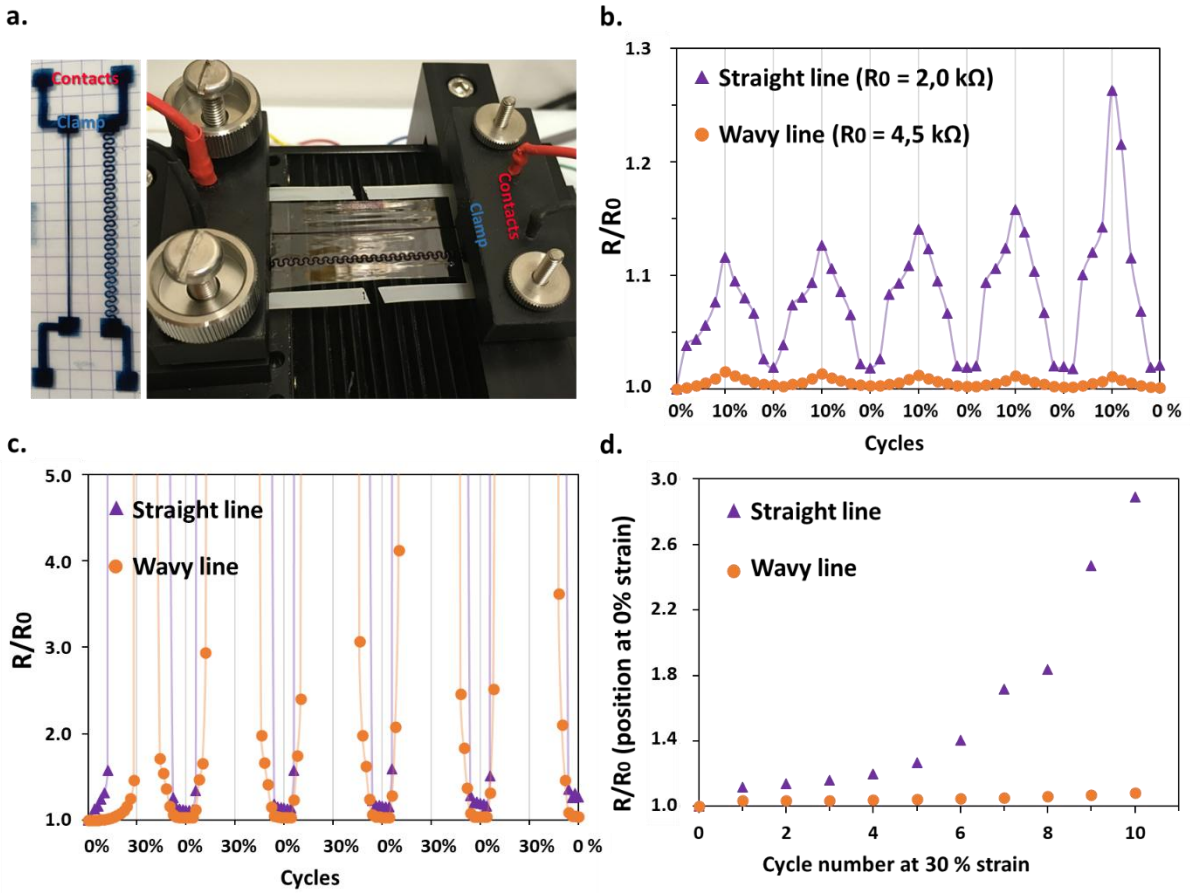

Figure 1. (a) Photographs of straight (left) and wavy (right) lines of *thick-PEDOT:OTf* (≈500 nm) on SEBS and the equipment used for the stretching tests. (b,c) Evolution of the resistance of *thick-PEDOT:OTf* lines (straight and wavy) on SEBS during 5 stretching cycles from 0% to (b) 10% and (c) 30% strain. (d) Resistance of the relaxed system as a function of the number of cycles at 30% strain.

There is a clear difference in the behavior of the two systems at 10% strain (**Figure 1**.b). The relative resistance of the wavy line increased by less than 1.5% in each cycle, while the relative resistance of the straight line had increased by 26% by the fifth cycle. An offset is still observed between the R/R0 profiles measured for the straight and wavy line at higher strains (**Figure 1**.c), but contact was lost in both cases at 30% strain. **Figure 1**.d shows that contrary to the cumulative increase observed for the straight line sample, the resistance of

the wavy sample returned to the initial value after each of 10 stretching cycles at 30% strain. This recovery of conductivity was observed after stretch/release cycles at all levels of strain from 10 to 80% (Figure S2). When measured 5 min after release from 80% strain, the resistance of the wavy line was less than 15% higher than at the start of the experiment. These first results seem promising for electrical switch applications.

Even with a wavy design, the *thick-PEDOT:OTf* films did not remain intact up to 30 % strain as required in stretchable electronics. In light of these disappointing results, the stretchability of *thick-PEDOT:Sulf (Sulf = sulfate counter-ion)* films was not studied, and we focused instead on the stretchability of *thin-PEDOT* films, which as well as being thin (≈ 35 nm thick), have a higher conductivity (> 3000 $S \cdot cm^{-1}$) and high transparency (> 80%). The properties of the different PEDOT films are compared in **Table S1**. Samples of *thin-PEDOT:OTf* and *thin-PEDOT:Sulf* were studied simultaneously . For these experiments, the SEBS substrate was fully coated by the polymers because the spin-coating method used offers no control over the location of the conductive material.

Figure 2.a,b shows the resistance profiles of the *thin-PEDOT:OTf* and *thin-PEDOT:Sulf* films over five cycles up to 10% and 30% strain. The strain cycling data for these films are presented in full in Figure S3. The conductivity of both films remained highly stable even at 30% strain, increasing by no more than 17% in the first cycle. Note that the resistance was highest at the maximal strain, but lowest (*i.e.* the conductivity was highest) at around 15% strain. A plausible explanation for this positive effect is that a small amount of strain increases chain alignment, which promotes current flow in the stretching direction. This hypothesis is discussed further below.

The resistance of the films was measured up to 100% strain, without any contact loss. **Figure 2**.c shows that both films preserved most of their electrical performance up to 50% strain, after which their resistance increased sharply, up to a maximum of 23-fold for *thin-PEDOT:OTf* and 17-fold for *thin-PEDOT:Sulf*. **Figure 2**.c also shows that the electrical properties of the *thin-PEDOT:OTf* film recovered better (R/R0 = 6 at 0% strain, after the 100% strain cycle) than those of the *thin-PEDOT:Sulf* film did (R/R0 = 8), even though the conductivity loss at 100% strain was greater for the *thin-PEDOT:OTf* film.

This may be the result of the type of cracks that form at high strain. **Figure 3** shows optical microscopy images of *thin-PEDOT:OTf, thin-PEDOT:Sulf* and *thin-PEDOT:PSS* (50 nm) films recorded during a 50% stretch/release cycle. The *thin-PEDOT:PSS* film was studied here as a reference material because of its widespread use and its chemical structure with a large polymeric counter-anion. In this film, wide cracks formed across the whole width of the sample, breaking the electrical path and preventing any mechanical healing. These observations are consistent with the very limited stretchability of this material. In the *thin-PEDOT:OTf* film, the first cracks, thin (≈3 µm) and short (≈20 µm), appeared at around 25–30% strain, but disappeared after stretching, the film being uniform again, without noticeable cracks. For *thin-PEDOT:Sulf*, the first cracks appeared above ~35% strain and were as long as the ones in *thin-PEDOT:OTf*, but wider (10 µm versus 6 µm) and fewer (see Table S2). Wider cracks remain after strain release, preventing any potential healing of the film. These results are in keeping with the lower resistance increase observed for the *thin-PEDOT:Sulf* film and the better recovery of the *thin-PEDOT:OTf* material.

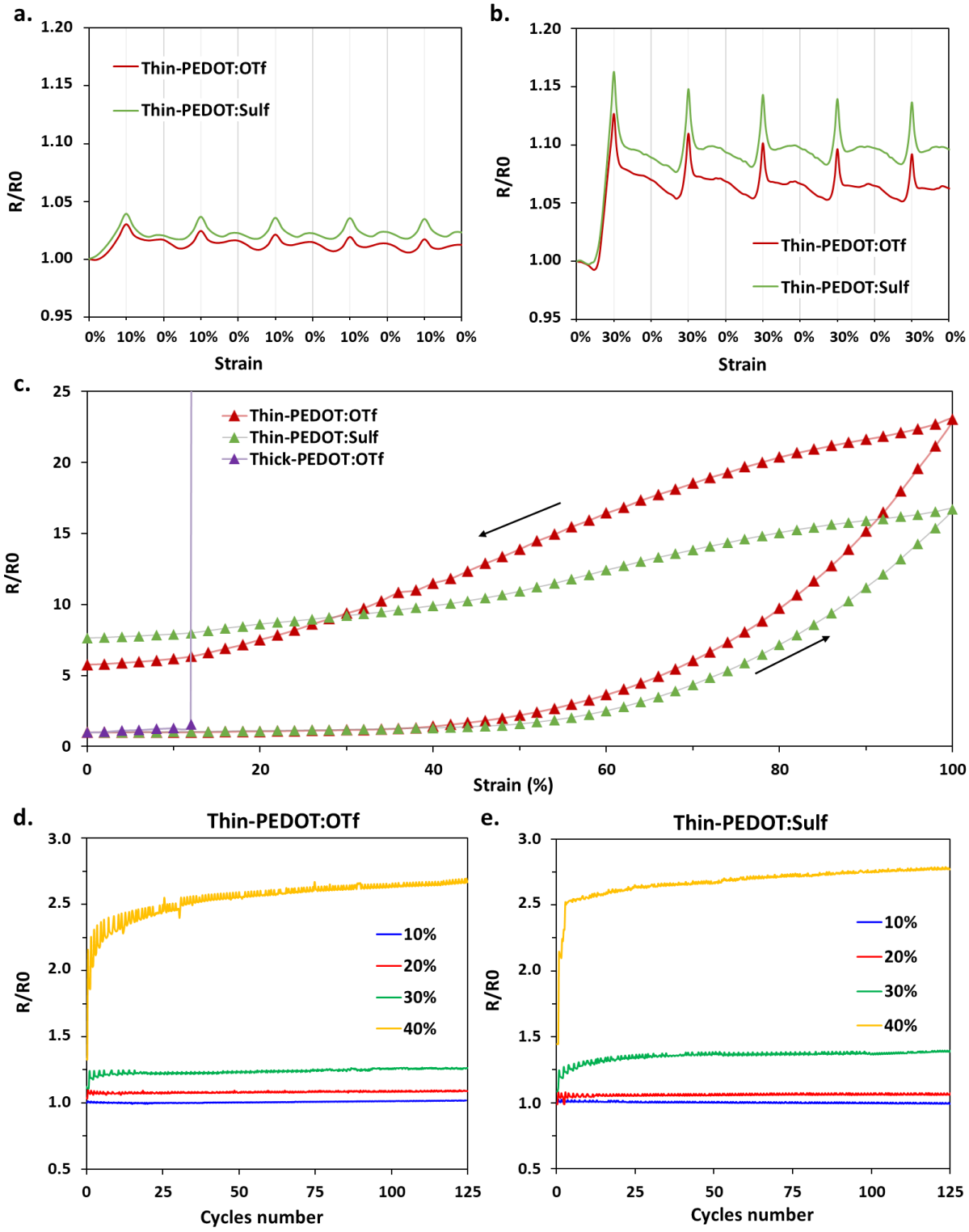

Figure 2. Evolution of the resistance of *thin-PEDOT:OTf* and *thin-PEDOT:Sulf* films during five cycles of stretching up to (a) 10% and (b) 30% strain. (c) Hysteresis of the resistance of *thin-PEDOT:OTf* (30–35 nm, red), *thin-PEDOT:Sulf* (30–35 nm, light green) and *thick-PEDOT:OTf* (500 nm, purple) on SEBS during stretching tests up to 100% strain. (e, d) Evolution of the resistance of (d) *thin-PEDOT:OTf* and (e) *thin-PEDOT:Sulf*, after 125 stretching-cycles at 10% (blue), 20% (red), 30% (dark green) and 40% (yellow) strain.

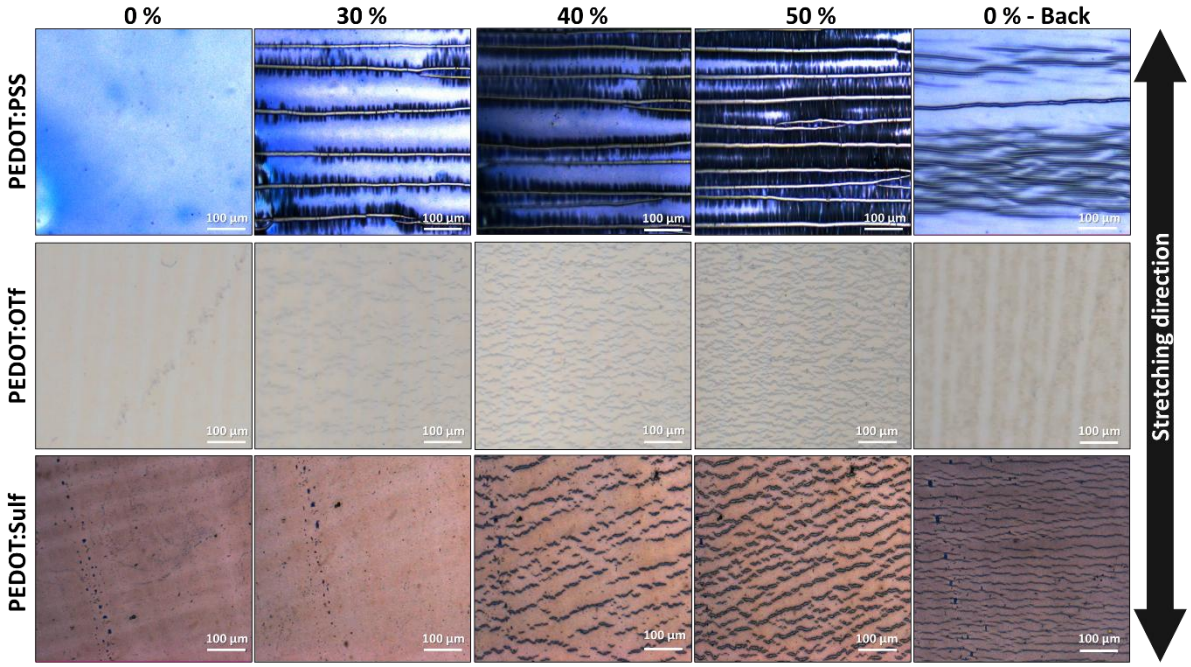

Figure 3. Optical micrographs of *thin-PEDOT:PSS, thin-PEDOT:OTf* and *thin-PEDOT:Sulf* films on SEBS during a stretch/release cycle (0%→50%→0% strain).

An important property of stretchable conductors is their electrical stability upon cycling. **Figure 2**.d,e shows that the electrical conductivity of both *thin-PEDOT:OTf* and *thin-PEDOT:Sulf* films remained highly stable over 125 cycles up to 30% strain, with relative resistance increases less than 26% for *thin-PEDOT:OTf* and less than 39% for *thin-PEDOT:Sulf*. At 40% strain however, the resistance more than doubled after just a few cycles, probably because of the formation of multiple cracks (**Figure 3**).

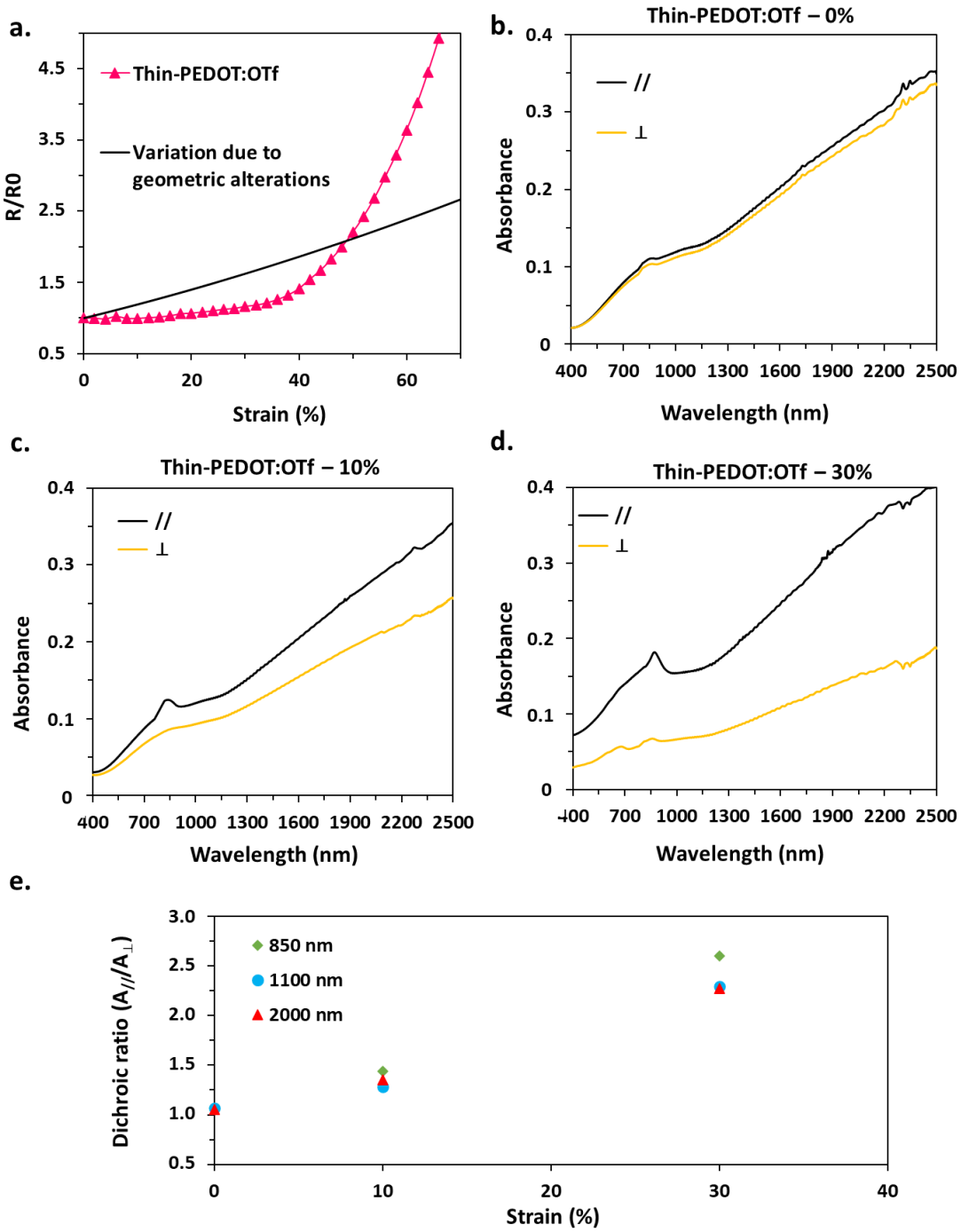

Figure 4. (a) Expected increase in relative resistance with increasing strain due to sample deformation (solid line) compared with experimental data for *thin-PEDOT:OTf* films on SEBS (magenta triangles). (b–d) UV-Vis-NIR absorbance parallel (//) and perpendicular (⊥) to the stretching direction in *thin-PEDOT:OTf* films chains for 0, 10 and 30 % strain, with PEDOT:OTf chain alignment evidenced by higher absorbance in the parallel than in the perpendicular direction. (f) Dichroic ratio (parallel absorbance / perpendicular absorbance) as a function of strain (%).

As described by **Equation 1**, if the conductivity of a material remains constant under strain, its resistance should increase because of sample deformation. **Figure 4**.a shows that up to 45% strain, the resistance measured for *thin-PEDOT:OTf* films was lower than the value

calculated with **Equation 1** and the Poisson ratios of SEBS and PEDOT. This means that the conductivity of *thin-PEDOT:OTf* films increases under stretching. Figure S5 displays the variation of the relative resistance of the material as a function of strain during stretching cycles. This effect has been reported previously and is ascribed here to chain alignment parallel to the stretching direction.[22,26] To confirm this hypothesis, we measured the absorbance parallel and perpendicular to the stretching direction of samples under 0, 10 and 30% strain by polarized UV-Vis-NIR spectroscopy (**Figure 4**.b-d). The optical anisotropy of the samples was quantified using the dichroic ratio, the ratio of the absorbances measured parallel and perpendicular to the stretching direction at a given wavelength. **Figure 4**.e shows that between 0% and 30% strain, this ratio increases linearly up to about 2.5, corresponding to an order parameter OP=(DR-1)/(DR+2) of 0.33 and indicating that the PEDOT chains are preferentially oriented parallel to the stretching direction. This explains the conductivity increase observed under strain, since charge carrier transport is known to be more efficient along chains than across them.[32] The origin of the peak around 800 nm in the spectra parallel to the stretching direction (**Figure 4**.c,d) is unclear. It may be a measurement artifact (due to the low absorbance of the films). It may also reflect a slight de-doping of the material (*i.e.* the chains becoming more neutral), suggesting that some counter-ions may be squeezed out during stretching, as described by Wang et al. for their PEDOT films doped and plasticized with ionic liquids.[22]

The results of these stretching tests indicate that *thin-PEDOT* films are suitable for electronic skin applications, such as heat patches, which are used in physiotherapy,[33] to reduce pain, [34,35] improve blood circulation[36] and accelerate healing.[37] As mentioned above, based on the level of stretching of the knee skin, the films must be able to sustain around 30% strain.[26,29]

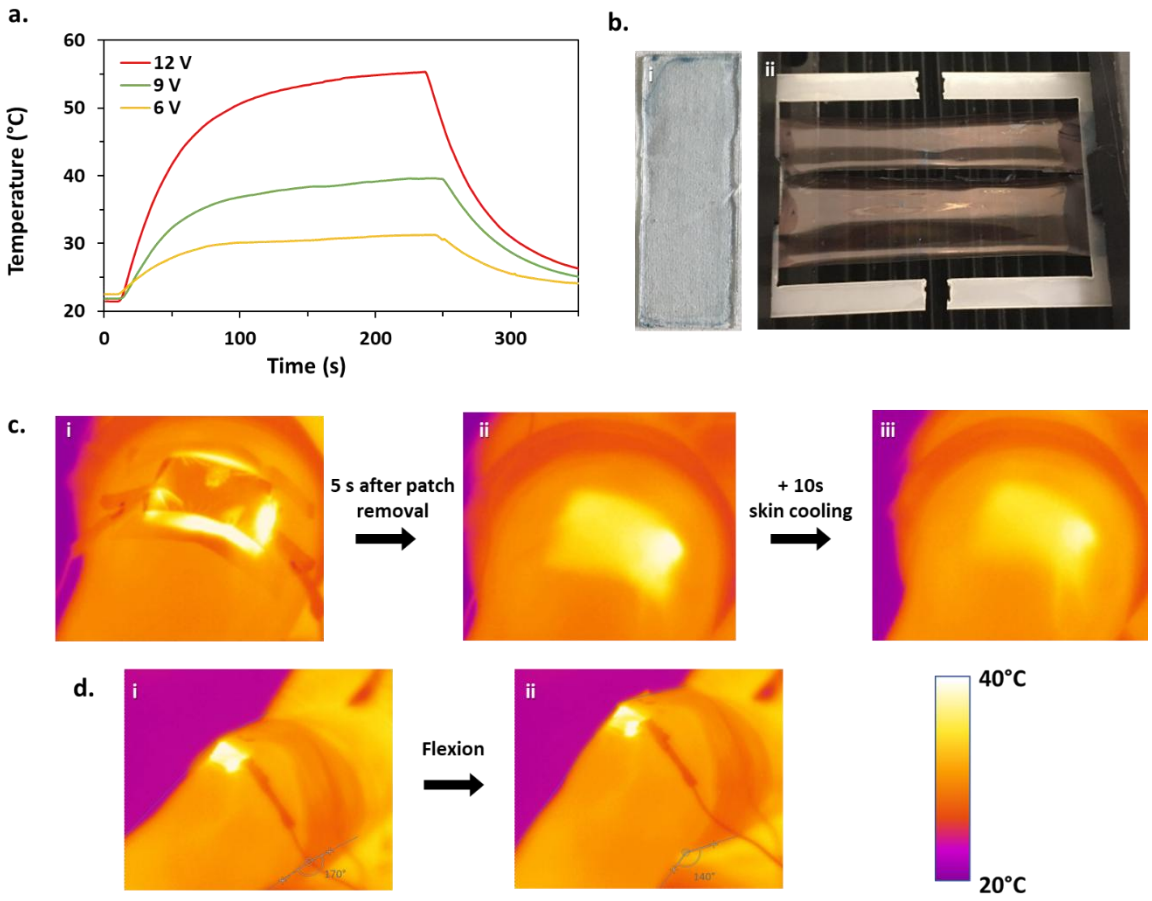

Figure 5. (a) Heating curves of PEDOT:OTf thin films on SEBS, at 6, 9 and 12 V. (b) Images of a thin-PEDOT:OTf patch (i) in resting position and (ii) during small (>10%) stretching. Infrared images of a PEDOT:OTf thermotherapy patch (8 × 5 cm^2) heated to 40°C (9 V applied) (c) on an extended knee, at rest, and (d) during knee flexion.

A 8 x 5 cm^2 thermotherapy patch was produced using *thin-PEDOT:OTf* on SEBS, with an average sheet resistance of 150 $\Omega.sq^{-1}$. The heating mechanism is the Joule effect, which depends on the resistance of the material ($P_{Joule} = U^2/R$).[38] Temperature profiles on the underside of the patch were measured at 6, 9 and 12 V (**Figure 5**.a), to ensure the temperature would not exceed 45°C when applied on the skin (to avoid any pain or burning; the temperature of the skin is generally about 30°C).[33,39] At 6 V the temperature after 100 s was only 30°C, while at 12 V the temperature reached 55°C. At 9V (≈20 mA), the temperature reached 40°C after 200s, and this was the voltage used in subsequent tests on skin. **Figure 5**.c shows infrared images recorded during and after application of the patch on the knee. The heating was uniform and persisted for a few seconds after removal. **Figure 5**.d shows that although slightly less heating was obtained during knee flexion, the patch

remained effective. This proof of concept highlights the potential of stretchable PEDOT based materials, in particular for the development of new stretchable transparent heaters.

II. Conclusion

The results presented in this paper demonstrate the intrinsic stretchability (up to 30% strain) of thin films of PEDOT-based materials with small counter-ions. Both *thin-PEDOT:OTf* and *thin-PEDOT:Sulf* films remain structurally sound up to 25–30% strain, and their conductivity remains remarkably stable over more than 100 cycles. Under limited amounts of strain (< 30%), polarized UV-Vis-NIR measurements (parallel and perpendicular to the stretching direction) show that the conductivity of the material is improved by chain alignment in the stretching direction. A thermotherapy patch produced with *thin-PEDOT:OTf* showed good temperature control (a stable 40°C at 9 V bias) and uniform heating across the surface. We think that the proposed approach could expand the range of materials for flexible transparent heaters and the use of stretchable conductive polymer materials in general.

Experimental section

Materials

3,4-Ethylenedioxythiophene (EDOT), N-methyl-2-pyrrolidone (NMP), iron(III) trifluoromethanesulfonate ($Fe(OTf)_3$), polyethylene glycol–polypropylene glycol–polyethylene glycol (PEG–PPG–PEG) Mw = 5800 $g.mol^{-1}$, ethylene glycol (EG) and toluene were obtained from Sigma-Aldrich. Anhydrous ethanol was purchased from CARLO ERBA Reagents. Polystyrene-b-poly(ethylene-butylene)-b-polystyrene (SEBS) Tuftec™ H1052 was graciously supplied by Asahi Kasei. PEDOT:PSS Clevios™ PH1000 was purchased from Heraeus.

Fabrication of PEDOT:OTf and PEDOT:Sulf films

The SEBS substrates were prepared by spin-coating a solution of SEBS (dissolved in toluene at a concentration of 200 $mg{\cdot}ml^{-1}$) on a glass substrate (10 × 10 cm^2) at 500 rpm for 1 min. The coated substrate was then heated on a hot plate at 70°C for 5 min.

Thick-PEDOT:OTf film was prepared as follows: $Fe(OTf)_3$ was dissolved at 63 $mg \cdot mL^{-1}$ in a solution containing 85.0 wt% ethanol, 10.0 wt% PEG– PPG–PEG and 5.0 wt% NMP. The solution was sonicated for 2 h. Then, 1 mL of the oxidizing solution was mixed with 10 µL of EDOT and directly sprayed (with a Colani manual spray-coater) on a SEBS substrate covered by a shadow mask. The resulting film was heated on a hot plate at 70°C for 10 min before being rinsed with ethanol (PEG-PPG-PEG is fully removed during this step) and dried again at 70°C. The *thick* film obtained had an average thickness of 500 nm.

Thin-PEDOT:OTf and *thin-PEDOT:Sulf* were prepared as follows: $Fe(OTf)_3$ was dissolved at 0.126 $mg \cdot mL^{-1}$ in a solution containing 72.25 wt% ethanol, 20.00 wt% PEG– PPG–PEG and 7.75 wt% NMP. The solution was sonicated for 2 h. Then, 0.25 mL of the oxidizing solution was mixed with 5 mL of EDOT and spin-coated onto the SEBS substrate at 4000 rpm for 30 s. The resulting film was heated on a hot plate at 70°C for 10 min before being rinsed with ethanol (PEG-PPG-PEG is fully removed during this step) and dried again at 70°C, yielding a *thin-PEDOT:OTf* film with an average thickness of 30–35 nm. To prepare *thin-PEDOT:Sulf* films, 0.1 M sulfuric acid was added dropwise on PEDOT:OTf film and left for 30 min before being removed (without rinsing). The film was then dried on a hot plate at 120°C for 30 min, yielding a *thin-PEDOT:Sulf* film with an average thickness of 30–35 nm.

To prepare *thin*-PEDOT:PSS films, SEBS substrate was plasma treated (120 W, 60 s) and CLEVIOS PH 1000 solution was sonicated for 1 min and directly spin-coated on SEBS at 1000 rpm for 45 s. The resulting film was heated on a hot plate at 120°C for 10 min.

Characterization

Sheet resistances (Rs) were measured at room temperature with a Loresta EP MCP-T360 resistivimeter. Samples were observed using an Infinite Focus optical microscope (×10 magnification). Infrared images were recorded with an Optris PI infrared camera. The temperature of the thermotherapy patch was measured with a type K thermocouple attached to the back of the device with Kapton® and was recorded with the software Picolog. A Varian Cary 5000 UV-Vis-NIR spectrophotometer with polarized incident light (spectral resolution of 1 nm) was used to probe the level of orientation in the films during stretching. The light polarization angle was measured with respect to the stretching direction (0°corresponding polarization parallel to the stretching direction and 90° to polarization perpendicular to the stretching direction).

Acknowledgements

The authors thank Frédéric Roux for his help for microscopy images.

References

(1) Gueye, M. N.; Carella, A.; Massonnet, N.; Yvenou, E.; Brenet, S.; Faure-Vincent, J.; Pouget, S.; Rieutord, F.; Okuno, H.; Benayad, A.; Demadrille, R.; Simonato, J.-P. Structure and Dopant Engineering in PEDOT Thin Films: Practical Tools for a Dramatic Conductivity Enhancement. *Chem. Mater.* **2016**, *28* (10), 3462–3468. https://doi.org/10.1021/acs.chemmater.6b01035.

(2) Schultheiss, A.; Carella, A.; Pouget, S.; Faure-Vincent, J.; Demadrille, R.; Revaux, A.; Simonato, J.-P. Water Content Control during Solution-Based Polymerization: A Key to Reach Extremely High Conductivity in PEDOT Thin Films. *J. Mater. Chem. C* **2020**, 10.1039.D0TC04899B. https://doi.org/10.1039/D0TC04899B.

(3) Schultheiss, A.; Gueye, M.; Carella, A.; Benayad, A.; Pouget, S.; Faure-Vincent, J.; Demadrille, R.; Revaux, A.; Simonato, J.-P. Insight into the Degradation Mechanisms of Highly Conductive Poly(3,4-Ethylenedioxythiophene) Thin Films. *ACS Appl. Polym. Mater.* **2020**, *2* (7), 2686–2695. https://doi.org/10.1021/acsapm.0c00301.

(4) Heydari Gharahcheshmeh, M.; Robinson, M. T.; Gleason, E. F.; Gleason, K. K. Optimizing the Optoelectronic Properties of Face-On Oriented Poly(3,4-Ethylenedioxythiophene) via Water-Assisted Oxidative Chemical Vapor Deposition. *Adv. Funct. Mater.* **2021**, *31* (14), 2008712. https://doi.org/10.1002/adfm.202008712.

(5) Shi, Y.; Zhou, Y.; Shen, R.; Liu, F.; Zhou, Y. Solution-Based Synthesis of PEDOT:PSS Films with Electrical Conductivity over 6300 S/Cm. *J. Ind. Eng. Chem.* **2021**, S1226086X21003105. https://doi.org/10.1016/j.jiec.2021.05.036.

(6) Fan, X.; Nie, W.; Tsai, H.; Wang, N.; Huang, H.; Cheng, Y.; Wen, R.; Ma, L.; Yan, F.; Xia, Y. PEDOT:PSS for Flexible and Stretchable Electronics: Modifications, Strategies, and Applications. *Adv. Sci.* **2019**, 1900813. https://doi.org/10.1002/advs.201900813.

(7) He, H.; Ouyang, J. Enhancements in the Mechanical Stretchability and Thermoelectric Properties of PEDOT:PSS for Flexible Electronics Applications. *Acc. Mater. Res.* **2020**, *1* (2), 146–157. https://doi.org/10.1021/accountsmr.0c00021.

(8) Heydari Gharahcheshmeh, M.; Gleason, K. K. Texture and Nanostructural Engineering of Conjugated Conducting and Semiconducting Polymers. *Mater. Today Adv.* **2020**, *8*, 100086. https://doi.org/10.1016/j.mtadv.2020.100086.

(9) Liu, Y.; Pharr, M.; Salvatore, G. A. Lab-on-Skin: A Review of Flexible and Stretchable Electronics for Wearable Health Monitoring. *ACS Nano* **2017**, *11* (10), 9614–9635. https://doi.org/10.1021/acsnano.7b04898.

(10) Sannicolo, T.; Lagrange, M.; Cabos, A.; Celle, C.; Simonato, J.-P.; Bellet, D. Metallic Nanowire-Based Transparent Electrodes for Next Generation Flexible Devices: A Review. *Small* **2016**, *12* (44), 6052–6075. https://doi.org/10.1002/smll.201602581.

(11) Qiu, J.; Wang, X.; Ma, Y.; Yu, Z.; Li, T. Stretchable Transparent Conductive Films Based on Ag Nanowires for Flexible Circuits and Tension Sensors. *ACS Appl. Nano Mater.* **2021**, *4* (4), 3760–3766. https://doi.org/10.1021/acsanm.1c00217.

(12) Lipomi, D. J.; Lee, J. A.; Vosgueritchian, M.; Tee, B. C.-K.; Bolander, J. A.; Bao, Z. Electronic Properties of Transparent Conductive Films of PEDOT:PSS on Stretchable Substrates. *Chem. Mater.* **2012**, *24* (2), 373–382. https://doi.org/10.1021/cm203216m.

(13) Kayser, L. V.; Lipomi, D. J. Stretchable Conductive Polymers and Composites Based on PEDOT and PEDOT:PSS. *Adv. Mater.* **2019**, 1806133. https://doi.org/10.1002/adma.201806133.
(14) Trung, T. Q.; Lee, N.-E. Materials and Devices for Transparent Stretchable Electronics. *J. Mater. Chem. C* **2017**, *5* (9), 2202–2222. https://doi.org/10.1039/C6TC05346G.
(15) Matsuhisa, N.; Chen, X.; Bao, Z.; Someya, T. Materials and Structural Designs of Stretchable Conductors. *Chem. Soc. Rev.* **2019**, *48* (11), 2946–2966. https://doi.org/10.1039/C8CS00814K.
(16) McCoul, D.; Hu, W.; Gao, M.; Mehta, V.; Pei, Q. Recent Advances in Stretchable and Transparent Electronic Materials. *Adv. Electron. Mater.* **2016**, *2* (5), 1500407. https://doi.org/10.1002/aelm.201500407.
(17) Kayser, L. V.; Lipomi, D. J. Stretchable Conductive Polymers and Composites Based on PEDOT and PEDOT:PSS. *Adv. Mater.* **2019**, *31* (10), 1806133. https://doi.org/10.1002/adma.201806133.
(18) Luo, R.; Li, H.; Du, B.; Zhou, S.; Zhu, Y. A Simple Strategy for High Stretchable, Flexible and Conductive Polymer Films Based on PEDOT:PSS-PDMS Blends. *Org. Electron.* **2020**, *76*, 105451. https://doi.org/10.1016/j.orgel.2019.105451.
(19) Savagatrup, S.; Chan, E.; Renteria-Garcia, S. M.; Printz, A. D.; Zaretski, A. V.; O'Connor, T. F.; Rodriquez, D.; Valle, E.; Lipomi, D. J. Plasticization of PEDOT:PSS by Common Additives for Mechanically Robust Organic Solar Cells and Wearable Sensors. *Adv. Funct. Mater.* **2015**, *25* (3), 427–436. https://doi.org/10.1002/adfm.201401758.
(20) Yeon, C.; Kim, G.; Lim, J. W.; Yun, S. J. Highly Conductive PEDOT:PSS Treated by Sodium Dodecyl Sulfate for Stretchable Fabric Heaters. *RSC Adv.* **2017**, *7* (10), 5888–5897. https://doi.org/10.1039/C6RA24749K.
(21) Oh, J. Y.; Kim, S.; Baik, H.-K.; Jeong, U. Conducting Polymer Dough for Deformable Electronics. *Adv. Mater.* **2016**, *28* (22), 4455–4461. https://doi.org/10.1002/adma.201502947.
(22) Wang, Y.; Zhu, C.; Pfattner, R.; Yan, H.; Jin, L.; Chen, S.; Molina-Lopez, F.; Lissel, F.; Liu, J.; Rabiah, N. I.; Chen, Z.; Chung, J. W.; Linder, C.; Toney, M. F.; Murmann, B.; Bao, Z. A Highly Stretchable, Transparent, and Conductive Polymer. *Sci. Adv.* **2017**, *3* (3), e1602076. https://doi.org/10.1126/sciadv.1602076.
(23) Teo, M. Y.; Kim, N.; Kee, S.; Kim, B. S.; Kim, G.; Hong, S.; Jung, S.; Lee, K. Highly Stretchable and Highly Conductive PEDOT:PSS/Ionic Liquid Composite Transparent Electrodes for Solution-Processed Stretchable Electronics. *ACS Appl. Mater. Interfaces* **2017**, *9* (1), 819–826. https://doi.org/10.1021/acsami.6b11988.
(24) Kee, S.; Kim, H.; Paleti, S. H. K.; El Labban, A.; Neophytou, M.; Emwas, A.-H.; Alshareef, H. N.; Baran, D. Highly Stretchable and Air-Stable PEDOT:PSS/Ionic Liquid Composites for Efficient Organic Thermoelectrics. *Chem. Mater.* **2019**, *31* (9), 3519–3526. https://doi.org/10.1021/acs.chemmater.9b00819.
(25) Li, P.; Sun, K.; Ouyang, J. Stretchable and Conductive Polymer Films Prepared by Solution Blending. *ACS Appl. Mater. Interfaces* **2015**, *7* (33), 18415–18423. https://doi.org/10.1021/acsami.5b04492.
(26) Dauzon, E.; Lin, Y.; Faber, H.; Yengel, E.; Sallenave, X.; Plesse, C.; Goubard, F.; Amassian, A.; Anthopoulos, T. D. Stretchable and Transparent Conductive PEDOT:PSS-Based Electrodes for Organic Photovoltaics and Strain Sensors Applications. *Adv. Funct. Mater.* **2020**, 2001251. https://doi.org/10.1002/adfm.202001251.
(27) He, H.; Zhang, L.; Guan, X.; Cheng, H.; Liu, X.; Yu, S.; Wei, J.; Ouyang, J. Biocompatible Conductive Polymers with High Conductivity and High Stretchability. *ACS Appl. Mater. Interfaces* **2019**, *11* (29), 26185–26193. https://doi.org/10.1021/acsami.9b07325.
(28) Gueye, M. N.; Carella, A.; Demadrille, R.; Simonato, J.-P. All-Polymeric Flexible Transparent Heaters. *ACS Appl. Mater. Interfaces* **2017**, *9* (32), 27250–27256. https://doi.org/10.1021/acsami.7b08578.
(29) Choi, S.; Park, J.; Hyun, W.; Kim, J.; Kim, J.; Lee, Y. B.; Song, C.; Hwang, H. J.; Kim, J. H.; Hyeon, T.; Kim, D.-H. Stretchable Heater Using Ligand-Exchanged Silver Nanowire Nanocomposite for

Wearable Articular Thermotherapy. *ACS Nano* **2015**, *9* (6), 6626–6633. https://doi.org/10.1021/acsnano.5b02790.
(30) Gercek, H. Poisson's Ratio Values for Rocks. *Int. J. Rock Mech. Min. Sci.* **2007**, *44* (1), 1–13. https://doi.org/10.1016/j.ijrmms.2006.04.011.
(31) Tahk, D.; Lee, H. H.; Khang, D.-Y. Elastic Moduli of Organic Electronic Materials by the Buckling Method. *Macromolecules* **2009**, *42* (18), 7079–7083. https://doi.org/10.1021/ma900137k.
(32) Noriega, R.; Rivnay, J.; Vandewal, K.; Koch, F. P. V.; Stingelin, N.; Smith, P.; Toney, M. F.; Salleo, A. A General Relationship between Disorder, Aggregation and Charge Transport in Conjugated Polymers. *Nat. Mater.* **2013**, *12* (11), 1038–1044. https://doi.org/10.1038/nmat3722.
(33) Lee, H. Effect of Heat and Cold on Tendon Flexibility and Force to Flex the Human Knee. *Med. Sci. Monit.* **2013**, *19*, 661–667. https://doi.org/10.12659/MSM.889145.
(34) Nadler, S. F.; Weingand, K.; Kruse, R. J. The Physiologic Basis and Clinical Applications of Cryotherapy and Thermotherapy for the Pain Practitioner. *Pain Physician* **2004**, *7* (3), 395–400.
(35) Cramer, H.; Baumgarten, C.; Choi, K.-E.; Lauche, R.; Saha, F. J.; Musial, F.; Dobos, G. Thermotherapy Self-Treatment for Neck Pain Relief—A Randomized Controlled Trial. *Eur. J. Integr. Med.* **2012**, *4* (4), e371–e378. https://doi.org/10.1016/j.eujim.2012.04.001.
(36) Lan, W.; Chen, Y.; Yang, Z.; Han, W.; Zhou, J.; Zhang, Y.; Wang, J.; Tang, G.; Wei, Y.; Dou, W.; Su, Q.; Xie, E. Ultraflexible Transparent Film Heater Made of Ag Nanowire/PVA Composite for Rapid-Response Thermotherapy Pads. *ACS Appl. Mater. Interfaces* **2017**, *9* (7), 6644–6651. https://doi.org/10.1021/acsami.6b16853.
(37) Barua, S. K.; Chowdhury, M. Z. A. Phonophoresis in Adhesive Capsulitis (Frozen Shoulder). *Chattagram Maa-O-Shishu Hosp. Med. Coll. J.* **2014**, *13* (1), 60–64.
(38) Papanastasiou, D. T.; Schultheiss, A.; Muñoz-Rojas, D.; Celle, C.; Carella, A.; Simonato, J.; Bellet, D. Transparent Heaters: A Review. *Adv. Funct. Mater.* **2020**, *30* (21), 1910225. https://doi.org/10.1002/adfm.201910225.
(39) Webb, P. Temperatures of Skin, Subcutaneous Tissue, Muscle and Core in Resting Men in Cold, Comfortable and Hot Conditions. *Eur. J. Appl. Physiol.* **1992**, *64* (5), 471–476.